




PAPER

Light-induced microfluidic chip based on shape memory gold nanoparticles/poly (vinyl alcohol) nanocomposites

To cite this article: Wenxin Wang *et al* 2018 *Smart Mater. Struct.* **27** 105047

View the [article online](#) for updates and enhancements.

Light-induced microfluidic chip based on shape memory gold nanoparticles/poly (vinyl alcohol) nanocomposites

Wenxin Wang^{1,2}, Xianbin Liu², Wei Xu¹, Hongqiu Wei¹, Yanju Liu³ , Yu Han⁴ , Peng Jin⁴, Hejun Du^{2,5} and Jinsong Leng^{1,5} 

¹ Center for Composite Materials and Structures, Harbin Institute of Technology, Harbin, 150080, People's Republic of China

² School of Mechanical and Aerospace Engineering, Nanyang Technological University, 639798, Singapore

³ Department of Astronautical Science and Mechanics, Harbin Institute of Technology, Harbin, 150080, People's Republic of China

⁴ Ultra-precision Optoelectronic Instrument Engineering Center, Harbin Institute of Technology, Harbin, 150080, People's Republic of China

E-mail: MHDU@ntu.edu.sg and lengjs@hit.edu.cn

Received 28 March 2018, revised 27 July 2018

Accepted for publication 6 September 2018

Published 21 September 2018



CrossMark

Abstract

A shape memory light-induced microfluidic technology is applied in preprogrammed microfluidic chip based on shape memory gold nanoparticles/poly (vinyl alcohol) nanocomposites. The shape memory gold nanoparticles/poly (vinyl alcohol) nanocomposites display excellent light-induced shape memory property with recovery ratio of nearly 100% in visible light. The crosslinked network of light-induced shape memory gold nanoparticles/poly (vinyl alcohol) nanocomposites forms by aldol reaction, esterification, and/or hydrogen bonding of poly (vinyl alcohol), glutaraldehyde, and gold nanoparticles. The light-induced shape memory mechanism of shape memory gold nanoparticles/poly (vinyl alcohol) nanocomposites is based on photothermal effect of gold nanoparticles and shape memory effect of poly (vinyl alcohol)-based shape memory polymer (SMP). In this report, a light-induced microfluidic microvalve is demonstrated based on the shape memory gold nanoparticles/poly (vinyl alcohol) nanocomposites. This research presents demonstration of the shape memory light-induced intelligent microfluidic chip. The light-induced SMP microfluidic microvalve would yield practical, physical, and technological advantages for disposable integrated microfluidic chip laboratories.

Keywords: photothermal effect, crosslinked network, light-induced microfluidic, shape memory polymer, nanocomposite

(Some figures may appear in colour only in the online journal)

1. Introduction

The SMP has the capacity to recover their permanent geometry from large-strain deformation by external stimuli such as heat, light, magnetic field, or electric current [1, 2]. The main advantages of SMP are low material and fabrication cost

coupled with simple operation and integration [3, 4]. The light-induced SMP can be remotely controlled without touching the material and topically activated without impacting other components [1, 3–5]. The challenge of light-induced SMP is how to convert light-induced shape memory effect (SME) between the molecular level and macroscopic movement. In one hand, the photo-reversible covalent crosslinking has been used as switch of SME under light

⁵ Authors to whom any correspondence should be addressed.

radiation [6]. In other hand, some functional nanofillers have been studied for light-induced SME [7–13]. The light-induced SMP can convert optical energy into mechanical work which has potential application in actuators, smart curtains, artificial muscles, and microelectromechanical systems [14–18]. One of the essential technologies for integrated microfluidic devices is microfluidic microvalve. Sugiura *et al* proposed a computer-controlled micropatterned on-chip fluid control strategies of a photoresponsive hydrogel sheet [19]. Although tremendous efforts have been devoted to developing various microvalves for microfluidic chip [20, 21], there are still many challenging issues to develop microfluidic systems for disposable integrated microfluidic chip laboratories [22–25].

The light-induced SMP composites have a promising application in novel microfluidic devices which is smaller scales by soft-lithography, low material and fabrication cost coupled with simple operation [3, 4]. A shape memory light-induced microfluidic chip can be remotely controlled and topically activated without impacting other components [1, 3–5], which have a promising application in microscale solution mixing, detection and control of chemical reactions with lower reagent or specimen consumption, preparing sample for mass spectrometry as well as biomolecule and biomedical cell separation [24, 26–31]. Lo *et al* reported an infrared light-responsive poly(N-isopropylacrylamide) hydrogel nanocomposite incorporating glycidyl methacrylate functionalized graphene oxide (GO–GMA) [32]. It is generally known that gold nanoparticles (AuNPs) can efficiently convert light energy into thermal energy [33, 34]. The photothermal effect of AuNPs can be used to trigger SME of the light-induced SMP nanocomposites [33–39]. Poly (vinyl alcohol)-based SMP has good thermally-driven shape memory property and ample hydroxyl group [40–43].

In this report, taking advantage of the photothermal effect of AuNPs and the SME of poly (vinyl alcohol)-based SMP, a shape memory light-induced microfluidic microvalve was demonstrated in preprogrammed microfluidic chip based on the shape memory gold nanoparticles/poly (vinyl alcohol) nanocomposites (AuNPs/PVA). When the light-induced microfluidic microvalve was exposed to light radiation, it can recover its original shape and then generate a negative pressure to inhale liquid samples into the microfluidic chip. The light-induced AuNPs/PVA microfluidic chip can achieve transduction at smaller scales, simpler, more reliable, and lower-cost actuation in a restricted environment [24–26].

2. Experimental section

2.1. Materials

Poly (vinyl alcohol) (PVA, $M_w = 85\,000\text{--}124\,000$, >99% hydrolysis), glutaraldehyde (GA, ~50% in H_2O), hydrogen tetrachloroaurate ($\text{HAuCl}_4 \cdot 3\text{H}_2\text{O}$) and sodium citrate ($\text{Na}_3\text{C}_6\text{H}_5\text{O}_7 \cdot 2\text{H}_2\text{O}$, for molecular biology, $\geq 99\%$) were bought from Sigma-Aldrich. Poly (dimethyl siloxane) (PDMS, 184) was purchased from Dow Corning. SU-8 negative tone photoresist was purchased from MicroChem

Corp. Cyanoacrylate adhesive was purchased from Join Leader Adhesive Co., Ltd. The ultrapure deionized water was used throughout the experiments.

2.2. Synthesis of light-induced shape memory gold nanoparticles/poly (vinyl alcohol) nanocomposites

HAuCl_4 solution (20 ml, 1 mM) was mixed with $\text{Na}_3\text{C}_6\text{H}_5\text{O}_7$ solution (2 ml, 1 wt%) and stirred for 5 min at 100°C . The gold nanoparticles (AuNPs) were claret. The light-induced shape memory AuNPs/PVA was prepared by PVA, GA, and AuNPs. 8 g PVA was dissolved in 100 ml ultrapure deionized water for 3 h at 98°C . The PVA solution was mixed with a certain amount of AuNPs at room temperature and then stirred for 1 h. The pH value of the solution was adjusted to 3.5 by adding hydrochloric acid, and then 3 ml GA was added in the solution. After stirring for 2 h, the bubble-free SMP precursor sol was obtained in vacuum and then poured into the mold at room temperature. It was dried for 48 h at room temperature and then for 3 h at 60°C and 24 h at 50°C in vacuum oven to obtain the light-induced shape memory AuNPs/PVA. The as-constructed nanocomposites were assigned as x wt% Au/PVA (x wt% is AuNPs content relative to nanocomposites weight: 0.1 wt% Au/PVA, 0.2 wt% Au/PVA, and 0.3 wt% Au/PVA, respectively). For a comparison, pure PVA-based SMP was assigned as PVA which was synthesized in the same conditions without AuNPs.

2.3. Fabrication of poly (dimethyl siloxane) microchannel

The PDMS microchannel was prepared by soft-lithography technique. The silicon wafer was washed by acetone and concentrated HNO_3 . The SU-8 negative tone photoresist was spin-coated onto silicon wafer. The silicon wafer was heated at 100°C to evaporate solvent, and then exposed in ultraviolet through the designed mask. The SU-8 negative tone photoresists selectively crosslinked in the exposed region at 110°C . The master was formed by removing the non-crosslinked SU-8 negative tone photoresists with SU-8 developer. The PDMS pre-polymer and the curing agent were blended at a certain mass ratio (10:1), removed bubble under vacuum, poured onto the master, and heated for 30 min at 80°C . The PDMS with designed microfluidic channels was stripped away the master. The height and width of microfluidic channels are $100\ \mu\text{m}$, respectively. The inlets were made by perforating holes at designed positions of PDMS microfluidic channels.

2.4. Characterization

The samples were examined by x-ray powder diffraction (XRD) with Empyrean XRD instrument (Panalytical, Holland). The Fourier transform infrared spectra (FTIR) of the samples were tested by Spectrum 100 Spectrometer (Perkin Elmer, America). Dynamic mechanical analysis (DMA) was carried out DMA/SDTA861e (Mettler-Toledo, Switzerland) in a tension mold. The transmission electron microscope (TEM) were performed on HITACHI H-7650 (HITACHI, Japan). The ultraviolet–visible (UV–vis) spectrum of the samples were tested by Shimadzu UV-3600 spectrometer

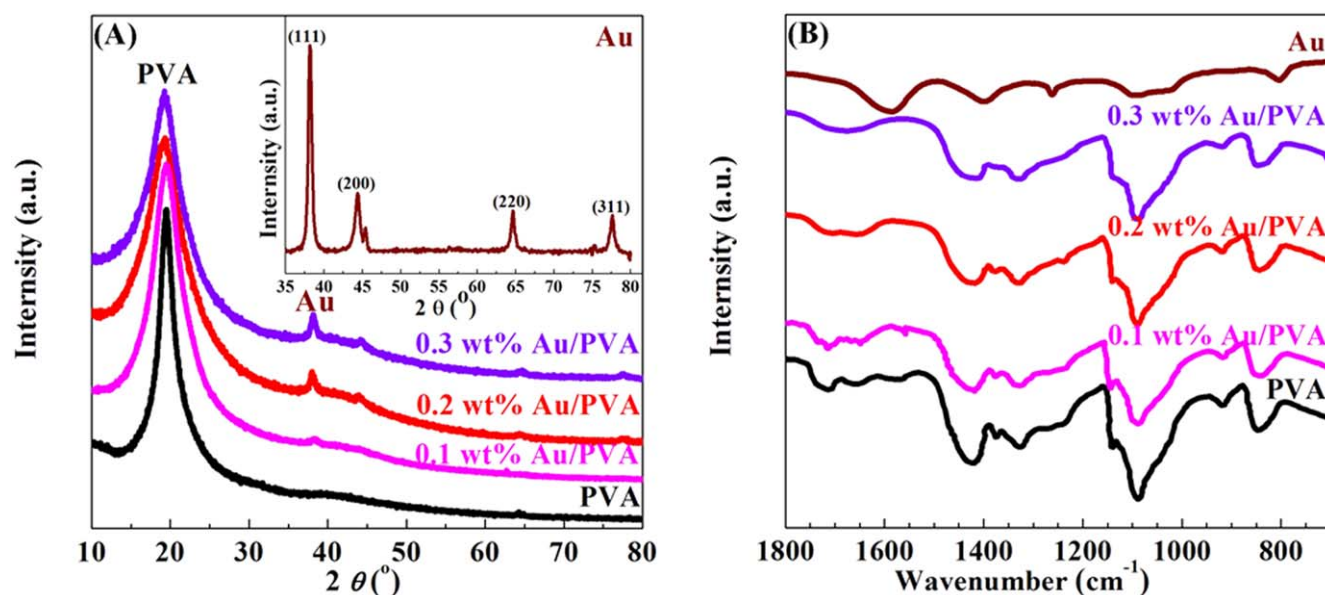


Figure 1. Crystalline structure and interaction. XRD patterns (A) and FTIR (B) of PVA, 0.1 wt% Au/PVA, 0.2 wt% Au/PVA, 0.3 wt% Au/PVA, and Au (inset).

(Shimadzu, Japan). Surface enhanced Raman scattering (SERS) analyses were performed with XploRA™ PLUS Raman spectromete (HORIBA, France). The temperature distribution was recorded with VarioCAM® hr thermal infrared camera system (Infra Tec, Germany).

3. Results and discussion

3.1. Characterization of light-induced shape memory AuNPs/PVA

The light-induced shape memory AuNPs/PVA was prepared via a simple solution co-blending method, such as descriptions in experimental section. XRD was used to examine the crystalline structure of the shape memory AuNPs/PVA. Figure 1(A) is XRD diffraction patterns of pure PVA-based SMP (designated as PVA), shape memory AuNPs/PVA (designated as 0.1 wt% Au/PVA, 0.2 wt% Au/PVA, 0.3 wt% Au/PVA), and gold nanoparticles (designated as Au). There is a broad peak at about $2\theta = 19.5^\circ$, which can be assigned to PVA. It is generally known that PVA is a crystalline polymer with abundant hydrogen bonding between nearby hydroxyl groups [44–46]. The peaks intensity at about 19.5° of PVA is reduced when AuNPs are added. It suggests that the AuNPs disturb the hydrogen bonding to decrease crystallinity. The XRD diffraction patterns of AuNPs at 38° , 44° , 65° , and 78° , corresponding to the (111), (200), (220), and (311) diffraction, is shown in figure 1(A-inset) [47]. The average crystalline size of AuNPs estimated by the Debye–Scherrer equation is approximately 12 nm. The XRD diffraction patterns of shape memory AuNPs/PVA reveal the diffraction peaks for PVA at 19.5° and predominantly Au (111) at 38° , confirming that AuNPs are doped into the PVA-based SMP matrix.

FTIR was aimed at identify the interaction between AuNPs and PVA-based SMP matrix. As shown in figure 1(B), the AuNPs exhibit characteristic absorptions of –OH bond bending vibration (1261 cm^{-1} , 1396 cm^{-1}) coupling with C–O bond stretching vibration, C–O bond stretching vibration of ester group (1020 cm^{-1} , 1095 cm^{-1}), C=O bond stretching vibration of carboxylate group in sodium citrate (1586 cm^{-1}), and hydrogen bond waging vibration (800 cm^{-1}) [48–50]. In the spectrum of PVA, the bands at 1234 cm^{-1} , 1324 cm^{-1} , 1375 cm^{-1} , and 1420 cm^{-1} are due to –OH and –CH bending vibration [46, 49]. The PVA also exhibits characteristic absorptions of C=O bond stretching vibration (1651 cm^{-1} , 1712 cm^{-1}), C–O bond stretching vibration (1088 cm^{-1}), and hydrogen bond waging vibration (845 cm^{-1}) [46, 50–60]. The –OH bond bending vibration peaks, C–O bond stretching vibration peak, and the C=O bond stretching vibration peaks weaken and shift to lower wavenumber with increasing AuNPs content in the shape memory AuNPs/PVA (figure 1(B)). The FTIR results reveal that there are hydrogen bonding and/or covalent bonding between oxygen-containing functional groups of AuNPs and PVA-based SMP matrix [52, 53]. Moreover, with increasing AuNPs content, the crosslink density of the shape memory AuNPs/PVA maybe increase since there are shorter chain length between crosslink point, and more reduced –OH group on the PVA molecular chain. Such bonding might decrease the crystallinity of PVA matrix. As a rule of thumb, the intensities of the 916 cm^{-1} and 1141 cm^{-1} bands are sensitive to the crystallinity of PVA matrix [49]. As shown in figure 1(B), the intensities of the 916 cm^{-1} and 1141 cm^{-1} bands weaken with increasing AuNPs content of the shape memory AuNPs/PVA. It suggests the crystallinity of PVA matrix reduce with increasing AuNPs content of the shape memory AuNPs/PVA, which match well with the XRD result. These results provide an evidence to support our previous statement.

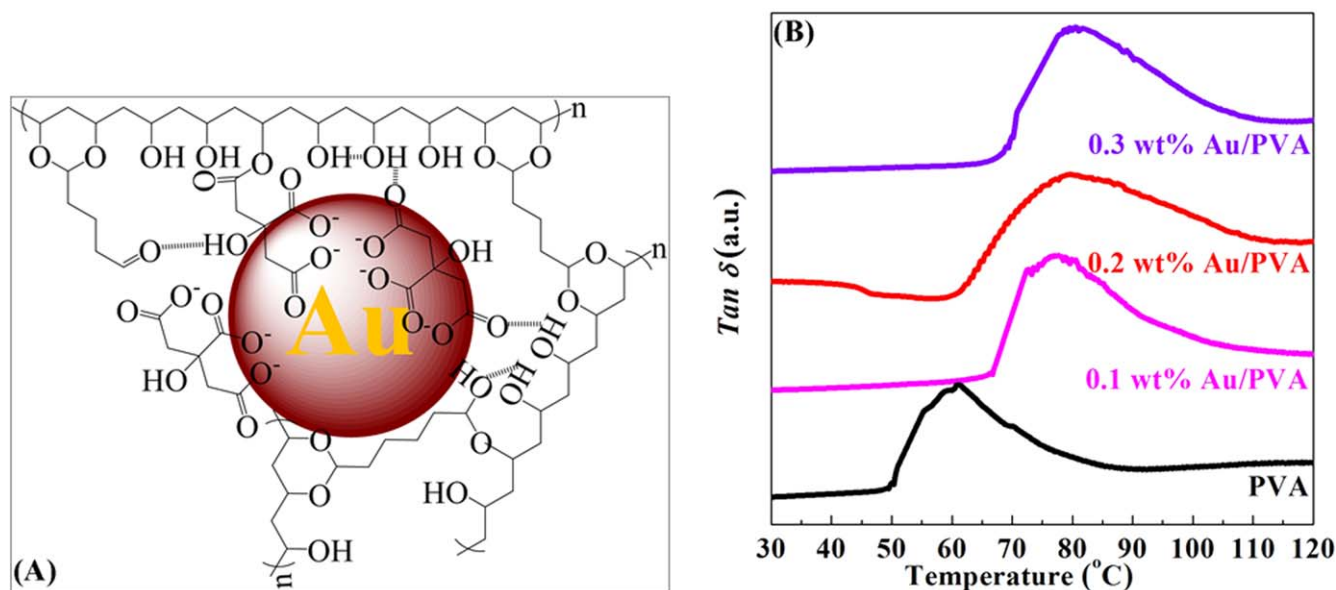


Figure 2. Crosslinked network and thermodynamic property. The crosslinked network of the shape memory AuNPs/PVA (A) and loss tangent ($\tan \delta$) versus temperature curves (B) of PVA, 0.1 wt% Au/PVA, 0.2 wt% Au/PVA, and 0.3 wt% Au/PVA.

The oxygen-containing functional groups of AuNPs can connect to PVA chain via hydrogen bonding and/or covalent bond. AuNPs and PVA matrix can stably co-exist in the shape memory AuNPs/PVA, and AuNPs content of the nanocomposites can be controlled.

As shown in figure 2(A), the crosslinked network of the shape memory AuNPs/PVA is constructed by aldol reaction, esterification, and/or hydrogen bonding of $-\text{OH}$ groups on the PVA molecular chains, two $\text{C}=\text{O}$ groups of glutaraldehyde, and/or oxygen-containing functional groups of AuNPs. The $-\text{OH}$ group on the PVA molecular chain can form hydrogen bonding, hemiacetal, and/or full acetal of six-membered ring with two $\text{C}=\text{O}$ groups of glutaraldehyde [41]. The polymer chains also can connect with oxygen-containing functional groups of AuNPs.

Figure 2(B) presents the evolution of loss tangent ($\tan \delta$) versus temperature for PVA and the shape memory AuNPs/PVA. In the graph, the $\tan \delta$ peak is attributed to the glass transition in amorphous domains of the PVA-based SMP matrix and the maximum $\tan \delta$ peak is designated as the transition temperature (T_{trans}) [58–65]. The external energy is effectively stored in the SMP below T_{trans} , and completely released above T_{trans} [52, 55]. The XRD and FTIR results confirm the crosslink density of the shape memory AuNPs/PVA maybe increase with increasing AuNPs content. As shown in figure 2(B), T_{trans} moves to higher temperature as AuNPs content increase, which can be attributed to stronger restriction of chain segments movement in amorphous region with crosslink density increasing [41]. As stated, T_{trans} of the shape memory AuNPs/PVA can be adjusted by AuNPs content.

To demonstrate the light-induced SME of the shape memory AuNPs/PVA, rectangular strip shape memory AuNPs/PVA was cut by laser for testing its light-induced shape recovery behavior. The straight bar shaped (permanent

shape) AuNPs/PVA was heated above $T_{trans} + 20^\circ\text{C}$ for 10 min in oven. After that, the shape memory AuNPs/PVA was bent into ‘V’-like shape. The bent shape memory AuNPs/PVA was fixed on the mandrel by external force and cooled to 25°C holding for 20 min. The bent shape memory AuNPs/PVA was left at room temperature for 24 h without apparent recovery. To investigate the light-induced shape recovery behavior of shape memory AuNPs/PVA, the bent shape memory AuNPs/PVA was exposed in visible light (0.2 W cm^{-2}). The shape recovery angle was designated as the angle between the two halves of bent shape memory AuNPs/PVA and directly read from protractor values. The shape recovery ratio (R_r) is quantified as follows:

$$R_r (\%) = \frac{A_r}{A_p} \times 100.$$

Here, A_p is initial angle and A_r is recovered angle.

The shape recovery ratio was plotted as a function of the light exposure time. In figure 3, the light-induced shape memory recovery ratio of shape memory AuNPs/PVA composites are nearly 100% in visible light. However, PVA has no apparent recovery in visible light. The light-induced shape memory recovery ratio of shape memory AuNPs/PVA composites increase with exposed time in visible light. Furthermore, the light-induced shape memory recovery ratio of the composites increase with AuNPs content at the same exposed time. The shape recovery ratio of shape memory AuNPs/PVA composites strongly depended on the AuNPs content. The 0.3 wt% shape memory AuNPs/PVA can recover its original shape from ‘V’-like shape (temporary shape) within 5 s in the visible light. This result confirms that shape memory AuNPs/PVA composites have good light-induced shape memory property and AuNPs play a key role in light-induced SME of the composites. The light-induced

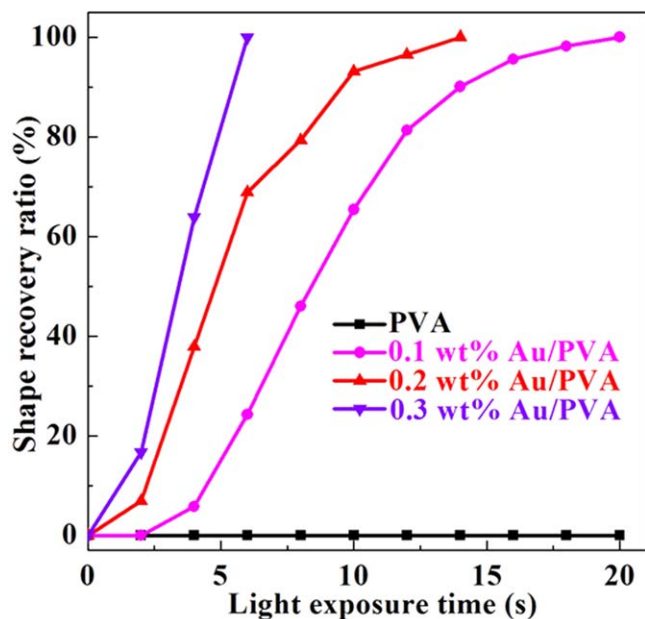


Figure 3. Shape memory property. Light-induced shape recovery behavior of Au/PVA with different Au content in visible light (0.2 W cm^{-2}): shape recovery ratio versus light exposure time.

shape memory property of the composites can be controlled by programming the AuNPs content.

3.2. Mechanism of light-induced SME

Herein, the light-induced SME mechanism of the AuNPs/PVA is studied. The morphology of AuNPs was examined by using TEM as shown in figure 4(A-inset). It can be seen that AuNPs are quasi spherical nanoparticle with good dispersibility and the average diameters of AuNPs are approximately 12 nm, which are consistent with FTIR and XRD

results. The optical absorption behavior of AuNPs was analyzed using UV-vis absorption spectrometer.

The quasi spherical AuNPs display an intense optical absorption band ($\lambda_{max} \approx 524 \text{ nm}$) in figure 4(A), which is attributed to surface plasmon resonance (SPR) effect of AuNPs [66]. The d electrons of AuNPs are free to travel through the material. When the incident light wavelength is much larger than the nanoparticle size, the resonant oscillations of conduction electrons at the interface between negative and positive permittivity are stimulated by the incident light [66, 67]. The enhanced electromagnetic field of metal nanoparticles can affect the local environment to enhance Raman signal of molecule on the metal nanoparticles surface [66]. From figure 4(B), the AuNPs have the strong band around 1583 cm^{-1} in SERS spectroscopy. These results clearly demonstrate that the as-prepared AuNPs have good SPR property.

The photothermal effect of PVA and the shape memory AuNPs/PVA can be assessed by thermal infrared camera system [68]. When the visible light irradiate on the sample, the temperature variation on the irradiated region of sample was detected by thermal infrared camera system. As shown in figure 5, the temperature of irradiated PVA and the irradiated shape memory AuNPs/PVA rises with exposed time in visible light. For pure PVA, there is no significant change. However, the temperature of the irradiated shape memory AuNPs/PVA can rises to above T_{trans} within 5 s. At the same time, the temperature of the irradiated shape memory AuNPs/PVA increase with increasing AuNPs content. AuNPs can transform light energy into thermal energy [33–39]. AuNPs are ideal functional component for light-induced SMP composites due to its good photothermal property, dispersibility, stability, and controllability. Therefore, the photothermal effect of AuNPs can be used to trigger SME of the light-induced SMP nanocomposites. The photothermal property of

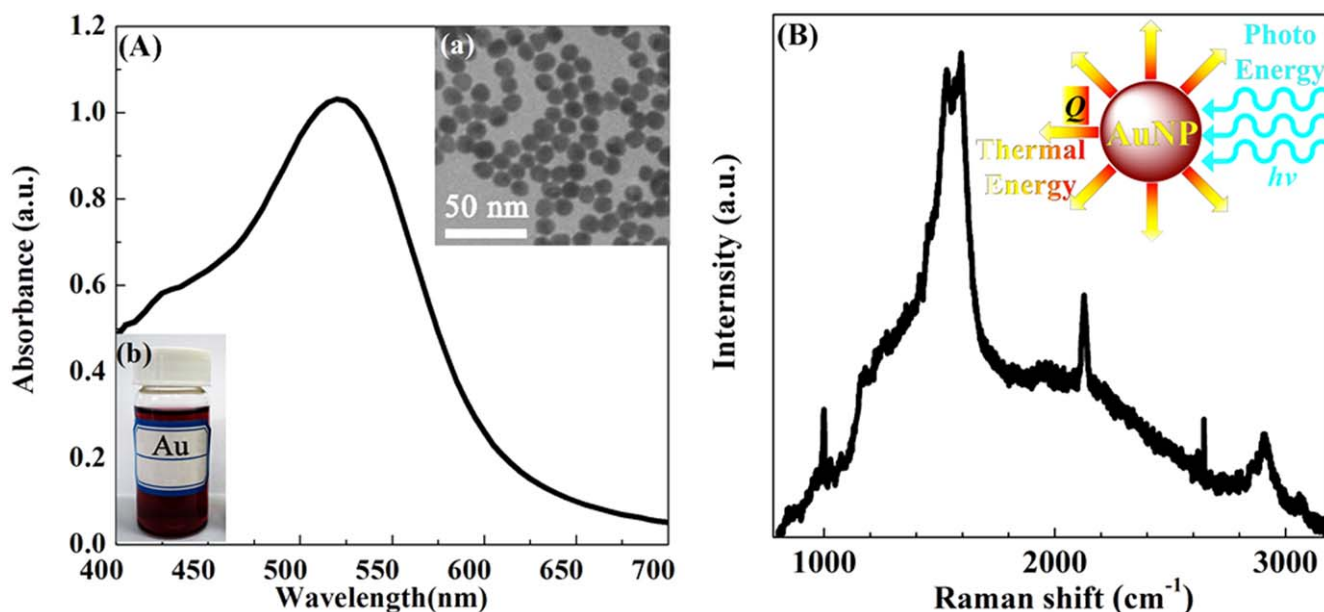


Figure 4. Optical performance and microstructure. UV-vis absorption spectrum of Au (inset: (a) TEM image of Au and (b) claret colloidal Au) (A) and SERS spectroscopy of Au (inset: photothermal effect of AuNPs) (B).

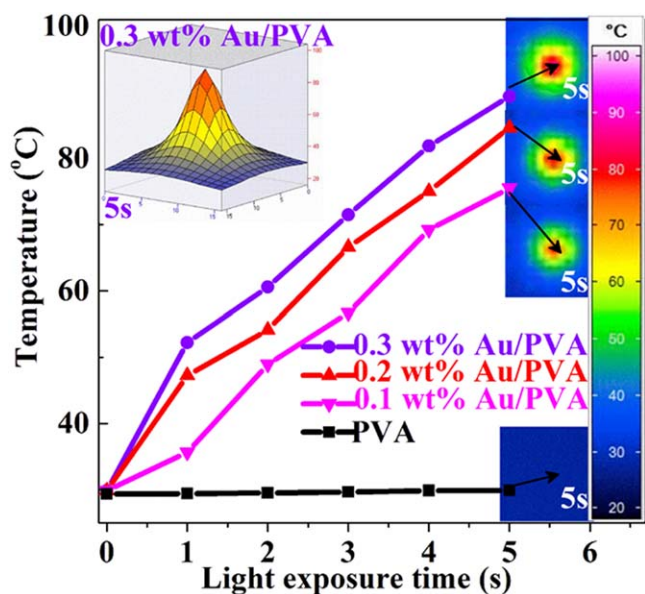


Figure 5. Photothermal effect in 5 s. Temperature versus light exposure time and infrared thermal images at 5 s of PVA, 0.1 wt% Au/PVA, 0.2 wt% Au/PVA, and 0.3 wt% Au/PVA (3D surface temperature distribution at 5 s) in visible light (0.2 W cm^{-2}).

AuNPs/PVA is attributed to good visible light absorption and SPR property of AuNPs as represented in figures 4 and 5. The light-induced SME of AuNPs/PVA is based on the photothermal effect of AuNPs and the SME of PVA-based SMP.

The temporary shape of SMP is deformed by extra force with frozen stress [4]. By external stimulus, the frozen stress will release to increase flexibility and result in recovering to original stress-free state of polymer chains [1–4]. PVA-based SMP has good thermally-driven shape memory property. The photothermal effect of AuNPs absorbs light energy and transforms it into thermal energy to trigger SME of the AuNPs/PVA in visible light irradiation. The macroscopic light-induced shape recovery property of shape memory AuNPs/PVA is observed in figure 3. These results imply that the light-induced shape memory AuNPs/PVA can convert light energy into mechanical energy with release strain energy. The polymer-based microfluidic systems is more inexpensive and disposable alternatives to early silicon-based and glass-based microfluidic systems [23]. It will enable the design and creation of disposable integrated microfluidic chip laboratories in an efficient and economical fashion. In conclusion, the light-induced shape memory AuNPs/PVA has promising application prospects in remotely controlling or topically activating microfluidic devices for disposable integrated microfluidic chip laboratories.

3.3. Light-induced microfluidic chip

The shape memory light-induced microfluidic chip is constructed with the light-induced AuNPs/PVA microfluidic microvalve, microfluidic channel, and glass wafer (figure 6). The light-induced AuNPs/PVA microfluidic microvalve can be predefined designate functions in the microfluidic chips. The polytetrafluoroethylene mold with bump structure was

used to prepare the light-induced AuNPs/PVA microfluidic microvalve with cavity volume in figure 6. To structurally preprogrammed (predefine) the light-induced SMP microfluidic microvalve, its morphology was changed to the flat surface by hot embossing machine with heat (above $T_{trans} + 20^\circ\text{C}$) and pressure (1 MPa) for 10 min and then keeping the pressure during the cooling process. The structurally preprogrammed light-induced AuNPs/PVA microfluidic microvalve can produce vacuum pressure via recovering the cavity volume (permanent shape) from the flat surface (temporary shape). Under light radiation, the preprogrammed light-induced AuNPs/PVA microfluidic microvalve recovers the cavity volume to generate negative pressure in the microfluidic chip. The liquid samples are sucked into the light-induced microfluidic chip by the vacuum pressure.

As shown in figure 6, the microfluidic channels include two inlets, channel, detection region, and a microcapsule in this research by soft-lithography. The detection region is smaller scales which have a promising application in micro-scale solution mixing, detection and control of chemical reactions with lower reagent or specimen consumption, preparing sample for mass spectrometry as well as biomolecule and biomedical cell separation [24, 26–31]. The transparent PDMS with designed microfluidic channels and the glass wafer with one connecting micropore of the microfluidic chip substrate were implemented bonding utilizing vacuum oxygen plasma. The connecting micropore of glass wafer can interconnect between the microfluidic channels and the light-induced microfluidic microvalve to inhale air and waste liquid samples into the microvalve. Finally, the light-induced SMP microfluidic microvalve was assembled with the bonded microfluidic chip substrate using cyanoacrylate adhesive.

To verify the performance of the light-induced shape memory AuNPs/PVA microfluidic chip, liquid samples (red ink and blue ink) were dropped on the inlets of microfluidic chip by pipette, respectively. The liquid samples kept on the inlets before light irradiation. As shown in figure 7, the liquid samples are inhaled into the light-induced microfluidic chip in visible light. The liquid samples take approximately 40 s to completely fill the microfluidic channels and arrive at the detection region. Under light irradiation, the preprogrammed light-induced shape memory AuNPs/PVA microfluidic microvalve can generate negative pressure for sucking the liquid samples via the shape transformation with releasing preprogrammed strain energy to perform mechanical work (figure 7). The light-induced SMP AuNPs/PVA microfluidic microvalve can be scaled down to the nanometer scale using nanoimprinting and hot-embossing manufacturing technologies to achieve miniaturization of chemical and biological analysis microfluidic laboratories.

Most chemical and biological analysis systems require microfluidic operations at room temperature. The light-induced method can reduce actuation power consumption without significantly affecting samples or other components, so it would be better than thermal, electrical and other driven methods. Moreover, the light-induced SMP microfluidic chip is a typical single-use device and can benefit avoiding the

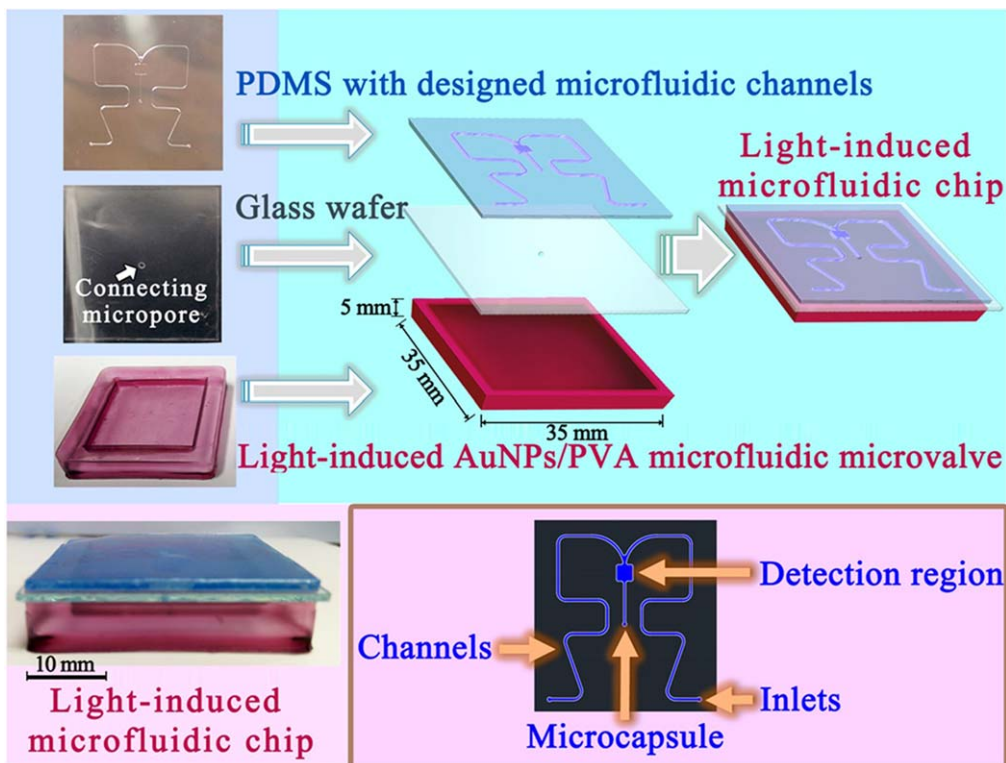


Figure 6. Design and packaging process of light-induced microfluidic chip. The transparent PDMS with designed microfluidic channels including two inlets, channel, detection region, and a microcapsule. The glass wafer with one connecting micropore. The light-induced AuNPs/PVA microfluidic microvalve with cavity volume.

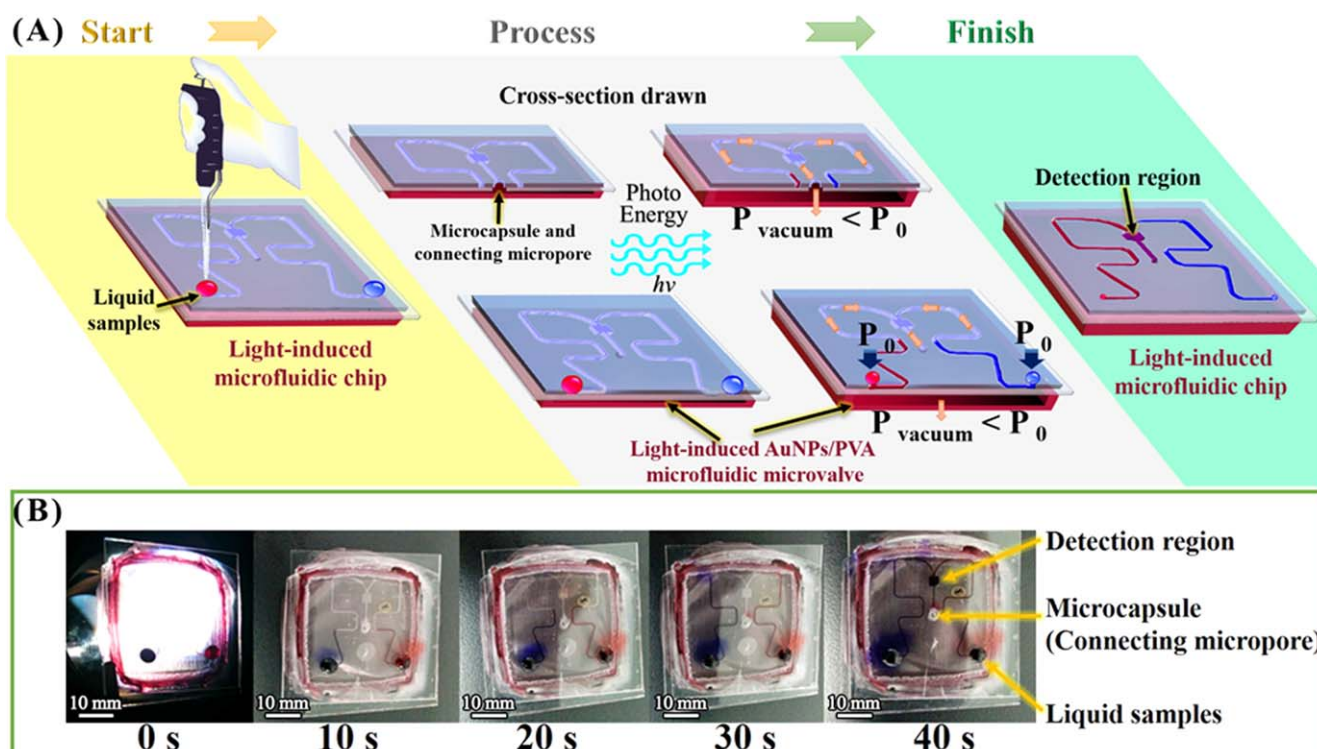


Figure 7. Design principle (A) and performance of light-induced microfluidic chip (B). The liquid samples (red ink and blue ink) stayed on the inlets before light irradiation. In visible light, the vacuum pressure (P_{vacuum}) was generated by recovering the cavity volume (permanent shape) from the flat surface (temporary shape) of the light-induced AuNPs/PVA microfluidic microvalve. Liquid samples were sucked into the microfluidic chip ($P_{vacuum} < P_0$).

cross-contamination in the chemical and biological analysis [19–23]. Therefore, the light-induced SMP AuNPs/PVA microfluidic device would be a promising alternative for disposable chemical and biological analysis microfluidic laboratories.

4. Conclusions

In this study, the shape memory light-induced shape memory AuNPs/PVA microfluidic chip was demonstrated. The shape memory AuNPs/PVA was synthesized by a simple solution co-blending method. The shape memory AuNPs/PVA exhibited excellent light-induced shape memory property in the visible light. The 0.3 wt% shape memory AuNPs/PVA can recover its original shape within 5 s in the visible light. The light-induced SME mechanism was attributed to the photothermal effect of AuNPs and the SME of PVA-based SMP. Under light irradiation, the preprogrammed light-induced shape memory AuNPs/PVA microfluidic microvalve generated negative pressure for inhaling the liquid samples via recovering the cavity volume (permanent shape) from the flat surface (temporary shape). This shape memory light-induced microfluidic chip is expected to contribute the practical application of disposable integrated microfluidic chip laboratories.

Acknowledgments

Project supported by the National Nature Science Foundation of China (Grant No. 11632005, 11672086), the Programme of Introducing Talents of Discipline to Universities (Grant No. B06010), and the Foundation for Innovative Research Groups of the National Natural Science Foundation of China (Grant No. 11421091), for which we are very grateful.

Author contributions statement

JL, HD, WW, and XL conceived and designed the research. WW, XL, XW, HW, and YH performed the experiments and measurements. WW and XL analyzed the data and discussed the results. JL, HD, YL, and PJ contributed to finalizing manuscript.


Additional information

Competing financial interests: the authors declare no competing financial interests.

ORCID iDs

Yanju Liu  <https://orcid.org/0000-0001-8269-1594>

Yu Han  <https://orcid.org/0000-0003-3539-9966>

Jinsong Leng  <https://orcid.org/0000-0001-5098-9871>

References

- [1] Leng J S, Lan X, Liu Y J and Du S Y 2011 Shape-memory polymers and their composites: stimulus methods and applications *Prog. Mater. Sci.* **56** 1077–135
- [2] Liu Y Y, Zhao J, Zhao L Y, Li W W, Zhang X Y and Zhang Z 2016 High performance shape memory epoxy/carbon nanotube nanocomposites *ACS Appl. Mater. Interfaces* **8** 311–20
- [3] Lendlein A and Langer R 2002 Biodegradable, elastic shape-memory polymers for potential biomedical applications *Science* **296** 1673–6
- [4] Wang W X, Liu Y J and Leng J S 2016 Recent developments in shape memory polymer nanocomposites: actuation methods and mechanisms *Coord. Chem. Rev.* **320–321** 38–52
- [5] Huang W M, Yang B, Zhao Y and Ding Z 2010 Thermo-moisture responsive polyurethane shape-memory polymer and composites: a review *J. Mater. Chem.* **20** 3367–81
- [6] Behl M and Lendlein A 2007 Shape-memory polymers *Mater. Today* **10** 20–8
- [7] Kohlmeyer R R, Lor M and Chen J 2012 Remote, local, and chemical programming of healable multishape memory polymer nanocomposites *Nano Lett.* **12** 2757–62
- [8] Liu Y, Boyles J K, Genzer J and Dickey M D 2012 Self-folding of polymer sheets using local light absorption *Soft Matter* **8** 1764–9
- [9] Leng J S, Wu X L and Liu Y J 2009 Infrared light-active shape memory polymer filled with nanocarbon particles *J. Appl. Polym. Sci.* **114** 2455–60
- [10] Liang J, Xu Y, Huang Y, Zhang L, Wang Y, Ma Y, Li F, Guo T and Chen Y 2009 Infrared-triggered actuators from graphene-based nanocomposites *J. Phys. Chem. C* **113** 9921–7
- [11] Yang Y, Pei Z, Zhang X, Tao L, Wei Y and Ji Y 2014 Carbon nanotube–vitimer composite for facile and efficient photo-welding of epoxy *Chem. Sci.* **5** 3486–92
- [12] Biyani M V, Foster E J and Weder C 2013 Light-healable supramolecular nanocomposites based on modified cellulose nanocrystals *ACS Macro Lett.* **2** 236–40
- [13] Meng H and Li G 2013 Reversible switching transitions of stimuli-responsive shape changing polymers *J. Mater. Chem. A* **1** 7838–65
- [14] Ikeda T, Mamiya J I and Yu Y L 2007 Photomechanics of liquid-crystalline elastomers and other polymers *Angew. Chem., Int. Ed.* **46** 506–28
- [15] Pei Z, Yang Y, Chen Q M, Terentjev E M, Wei Y and Ji Y 2014 Mouldable liquid-crystalline elastomer actuators with exchangeable covalent bonds *Nat. Mater.* **13** 36–41
- [16] Li M, Keller P, Li B, Wang X G and Brunet M 2003 Light-driven side-on nematic elastomer actuators *Adv. Mater.* **15** 569–527
- [17] Lu H B, Yao Y T, Huang W M, Leng J S and Hui D 2014 Significantly improving infrared light-induced shape recovery behavior of shape memory polymeric nanocomposite via a synergistic effect of carbon nanotube and boron nitride *Composites B* **62** 256–61
- [18] Yu L and Yu H F 2015 Light-powered tumbler movement of graphene oxide/polymer nanocomposites *ACS Appl. Mater. Interfaces* **7** 3834–9
- [19] Sugiura S, Szilágyi A, Sumaru K, Hattori K, Takagi T, Filipcsei G, Zrínyi M and Kanamori T 2009 On-demand microfluidic control by micropatterned light irradiation of a photoresponsive hydrogel sheet *Lab Chip* **9** 196–8
- [20] Shoji S and Esashi M 1994 Microflow devices and systems *J. Micromech. Microeng.* **4** 157–71
- [21] Oh K W and Ahn C H 2006 A review of microvalves *J. Micromech. Microeng.* **16** R13–39

- [22] Becker H and Gärtner C 2000 Polymer microfabrication methods for microfluidic analytical applications *Electrophoresis* **21** 12–26
- [23] Fiorini G S and Chiu D T 2005 Disposable microfluidic devices: fabrication, function, and application *Biotechniques* **38** 429–46
- [24] Srivastava S, Solanki P R, Kaushik A, Ali M A, Srivastava A and Malhotra B D 2011 A self assembled monolayer based microfluidic sensor for urea detection *Nanoscale* **3** 2971–7
- [25] Goral V N, Zaytseva N V and Baeumner A J 2006 Electrochemical microfluidic biosensor for the detection of nucleic acid sequences *Lab Chip* **6** 414–21
- [26] Li L, Lv X Q, Ostrovidov S, Shi X T, Zhang N and Liu J 2014 Biomimetic microfluidic device for *in vitro* antihypertensive drug evaluation *Mol. Pharmaceutics* **11** 2009–15
- [27] Whitesides G M and Stroock A D 2001 Flexible methods for microfluidics *Phys. Today* **54** 42–8
- [28] Ren K N, Zhou J H and Wu H K 2013 Materials for microfluidic chip fabrication *Acc. Chem. Res.* **46** 2396–406
- [29] Jackson W C, Tran H D, O'Brien M J, Rabinovich E and Lopez G P 2001 Rapid prototyping of active microfluidic components based on magnetically modified elastomeric materials *J. Vac. Sci. Technol.* **19** 596–9
- [30] Yan S Q, Zhang X, Dai X F, Feng X J, Du W and Liu B F 2016 Rhipsalis (cactaceae)-like hierarchical structure based microfluidic chip for highly efficient isolation of rare cancer cells *ACS Appl. Mater. Interfaces* **8** 33457–63
- [31] Xu Z Y, Li E C, Guo Z, Yu R F, Hao H L, Xu Y T, Sun Z, Li X C, Lyu J X and Wang Q 2016 Design and construction of a multi-organ microfluidic chip mimicking the *in vivo* microenvironment of lung cancer metastasis *ACS Appl. Mater. Interfaces* **8** 25840–7
- [32] Lo C W, Zhu D F and Jiang H R 2011 An infrared-light responsive graphene-oxide incorporated poly(N-isopropylacrylamide) hydrogel nanocomposite *Soft Matter* **7** 5604–9
- [33] Maity S, Bochinski J R and Clarke L I 2012 Metal nanoparticles acting as light-activated heating elements within composite materials *Adv. Funct. Mater.* **22** 5259–70
- [34] Zhang H, Fortin D, Xia H and Zhao Y 2013 Fast optical healing of crystalline polymers enabled by gold nanoparticles *Macromol. Rapid Commun.* **34** 1742–6
- [35] Zhang H J and Zhao Y 2013 Polymers with dual light-triggered functions of shape memory and healing using gold nanoparticles *ACS Appl. Mater. Interfaces* **5** 13069–75
- [36] Hribar K C, Lee M H, Lee D and Burdick J A 2011 Enhanced release of small molecules from near-infrared light responsive polymer–nanorod composites *ACS Nano* **5** 2948–56
- [37] Zhang H J, Xia H S and Zhao Y 2014 Light-controlled complex deformation and motion of shape-memory polymers using a temperature gradient *ACS Macro Lett.* **3** 940–3
- [38] Zhang H J, Zhang J M, Tong X, Ma D L and Zhao Y 2013 Light polarization-controlled shape-memory polymer/gold nanorod composite *Macromol. Rapid Commun.* **34** 1575–9
- [39] Zheng Y W, Li J, Lee E and Yang S 2015 Light-induced shape recovery of deformed shape memory polymer micropillar arrays with gold nanorods *RSC Adv.* **5** 30495–9
- [40] Hiral T, Maruyama H, Suzuki T and Hayashi S 1992 Shape memorizing properties of a hydrogel of poly (vinyl alcohol) *J. Appl. Polym. Sci.* **45** 1849–55
- [41] Du H Y and Zhang J H 2010 Shape memory polymer based on chemically cross-linked poly(vinyl alcohol) containing a small number of water molecules *Colloid Polym. Sci.* **288** 15–24
- [42] Seydou M, Teyssandier J, Battaglini N, Kenfack G T, Lang P, Tielens F, Maurel F and Diawara B 2014 Characterization of NTCDI supramolecular networks on Au(111); combining STM, IR and DFT calculations *RSC Adv.* **4** 25698–708
- [43] Subramanyam U and Kennedy J P 2009 PVA Networks grafted with PDMS branches *J. Polym. Sci.* **47** 5272–7
- [44] Du H Y, Zhou T, Zhang J H and Liu X Y 2010 Moving-window two-dimensional correlation infrared spectroscopy study on structural variations of partially hydrolyzed poly (vinyl alcohol) *Anal. Bioanal. Chem.* **397** 3127–32
- [45] Du H Y and Zhang J H 2012 The synthesis of poly (vinyl cinnamates) with light-induced shape fixity properties *Sensors Actuators A* **179** 114–20
- [46] Gonzalez J S, Ludueña L N, Ponce A and Alvarez V A 2014 Poly(vinyl alcohol)/cellulose nanowhiskers nanocomposite hydrogels for potential wound dressings *Mater. Sci. Eng. C* **34** 54–61
- [47] Adhyapak P V, Singh N, Vijayan A, Aiyer R C and Khanna P K 2007 Single mode waveguide properties of M-NA doped Au/PVA nano-composites: synthesis, characterization and studies *Mater. Lett.* **61** 3456–61
- [48] Chen Y, Geng J Q, Zhuang Y X, Zhao J, Chu L Q, Luo X X, Zhao Y and Guo Y W 2016 Preparation of the chitosan grafted poly (quaternary ammonium)/Fe₃O₄ nanoparticles and its adsorption performance for food yellow 3 *Carbohydrate Polym.* **152** 327–36
- [49] Sugiura K, Hashimoto M, Matsuzawa S and Yamaura K 2001 Influence of degree of crystallinity and syndiotacticity on infrared spectra of solid PVA *J. Appl. Polym. Sci.* **82** 1291–8
- [50] Wang W X, Lu H B, Liu Y J and Leng J S 2014 Sodium dodecyl sulfate/epoxy composite: water-induced shape memory effect and its mechanism *J. Mater. Chem. A* **2** 5441–9
- [51] Wang J C, Wang X B, Xu C H, Zhang M and Shang X P 2011 Preparation of graphene/poly (vinyl alcohol) nanocomposites with enhanced mechanical properties and water resistance *Polym. Int.* **60** 816–22
- [52] Du F P, Ye E Z, Tang C Y, Ng S P, Zhou X P and Xie X L 2013 Microstructure and shape memory effect of acidic carbon nanotubes reinforced polyvinyl alcohol nanocomposites *J. Appl. Polym. Sci.* **129** 1299–305
- [53] Qi X D, Yao X L, Deng S, Zhou T N and Fu Q 2014 Water-induced shape memory effect of graphene oxide reinforced polyvinyl alcohol nanocomposites *J. Mater. Chem. A* **2** 2240–9
- [54] Ram S and Mandal T K 2004 Photoluminescence in small isotactic, atactic and syndiotactic PVA polymer molecules in water *Chem. Phys.* **303** 121–8
- [55] Delnoye D A P, Sijbesma R P, Vekemans J J M and Meijer E W 1996 π -Conjugated oligomers and polymers with a self-assembled ladder-like structure *J. Am. Chem. Soc.* **118** 8717–8
- [56] Du H Y, Song Z, Wang J J, Liang Z H, Shen Y H and You F 2015 Microwave-induced shape-memory effect of siliconcarbide/poly (vinyl alcohol) composite *Sensors Actuators A* **228** 1–8
- [57] Li H B, Zhang W K, Xu W Q and Zhang X 2000 Hydrogen bonding governs the elastic properties of poly (vinyl alcohol) in water: single-molecule force spectroscopic studies of PVA by AFM *Macromolecule* **33** 465–9
- [58] Uda A, Morita S and Ozaki Y 2013 Thermal degradation of a poly(vinyl alcohol) film studied by multivariate curve resolution analysis *Polymer* **54** 2130–7
- [59] Zheng P and Ling X K 2007 A thermal degradation mechanism of polyvinyl alcohol/silica nanocomposites *Polym. Degrad. Stab.* **92** 1061–71
- [60] Holland B J and Hay J N 2001 The thermal degradation of poly (vinyl alcohol) *Polymer* **42** 6775–83
- [61] Ohki T, Ni Q Q, Ohsako N and Iwamoto M 2004 Mechanical and shape memory behavior of composites with shape memory polymer *Composites A* **35** 1065–73

- [62] Cuq B, Gontard N and Guilbert S 1997 Thermal properties of fish myofibrillar protein-based films as affected by moisture content *Polymer* **38** 2399–405
- [63] Tsai Y, Tai C, Tsai S and Tsai F 2008 Shape memory effects of poly (ethylene terephthalate-co-ethylene succinate) random copolymers *Eur. Polym. J.* **44** 550–4
- [64] Krumova M, López D, Benavente R, Mijangos C and Pereña J M 2000 Effect of crosslinking on the mechanical and thermal properties of poly(vinyl alcohol) *Polymer* **41** 9265–72
- [65] Liu G Q, Guan C L, Xia H S, Guo F Q, Ding X B and Peng Y X 2006 Novel shape-memory polymer based on hydrogen bonding *Macromol. Rapid Commun.* **27** 1100–4
- [66] Sujit K G and Tarasankar P 2007 Interparticle coupling effect on the surface plasmon resonance of gold nanoparticles: from theory to applications *Chem. Rev.* **107** 4797–862
- [67] Clark H A, Campagnola P J, Wuskell J P, Lewis A and Loew L M 2000 Second harmonic generation properties of fluorescent polymer-encapsulated gold nanoparticles *J. Am. Chem. Soc.* **122** 10234–5
- [68] Wang W X, Liu D Y, Liu Y J, Leng J S and Bhattacharyya D 2015 Electrical actuation properties of reduced graphene oxide paper/epoxy-based shape memory composites *Compos. Sci. Technol.* **106** 20–4